11-3-2016

Cracking Potential and Temperature Sensitivity of Metakaolin Concrete

Andrew Robert Williams
University of South Florida, andrewrobert@mail.usf.edu

Cracking Potential and Temperature Sensitivity of Metakaolin Concrete

by

Andrew Williams

A thesis submitted in partial fulfillment
of the requirements for the degree of
Master of Science in Civil Engineering
Department of Civil and Environmental Engineering
College of Engineering
University of South Florida

Major Professor: Abla Zayed, Ph.D.
Rajan Sen, Ph.D.
Kyle Riding, Ph.D.

Date of Approval:
October 26, 2016

Keywords: Cracking Risk, Temperature Reactivity, Pore Distribution, Phase Transformation

DEDICATION

I would like to dedicate this work to my family and friends. Without their love and support I wouldn’t be who I am or where I am today.

ACKNOWLEDGEMENTS

I would like to thank all of the people that have helped me succeed in this accomplishment. I would like to express my gratitude towards Dr. Zayed for being the academic advisor that I needed, providing support in a conglomeration of ways and providing guidance throughout my academic journey. I would also like to thank Dr. Riding for the time, patience and knowledge he has provided me over the years. I would also like to voice my appreciation to Dr. Sen for the many life and academic lessons taught me inside and out of the classroom.

I express my deepest appreciation to many people: Natallia, Victor, Tom, Dan, Tony, Jeremy, Reza, Ananaya, Dhanushika, Ahmed, Josh, Yuriy and Billy. All of you have been wonderful friends and I truly treasure our time together. Thank you Natallia and Yuriy for helping me learn so much and for all of the laughs we've shared. Victor, thank you for always being willing to help and making the workplace filled with fun. Thank you Tom for being an outstanding mentor, although the time was short it was filled with hard work and amusement. I can only hope that I'll inspire others as well as you've trained me. Even though I never worked with you Dan, thank you for answering so many questions of mine and being an inspiration to strive to be like. Tony, thank you for helping me with experiments and teaching me many more Thank you Jeremy, Billy and Josh for helping with running and cleaning all the experiments, amongst all the problem solving, construction assistance and laughs. Ananya, Ahmed and Dhanushika, thank you for eagerness to learn and for helping with everything work and school related you've done. I would also like to thank the FDOT for their financial support as well as W.R. Grace for the materials donated in order to conduct this experimental work.

TABLE OF CONTENTS

LIST OF TABLES

LIST OF FIGURES

ABSTRACT[1]

Metakaolin is a pozzolanic material with the potential to reduce permeability and chloride ingress; however, quantification of the effects of metakaolin use on the cracking sensitivity of concrete mixtures is needed to ensure that these improvements in performance are not compromised. This study was conducted to investigate the early age cracking potential due to restraint stresses from incorporating metakaolin in concrete. Calorimetry testing showed that metakaolin was more sensitive to temperature than mixtures with only Portland cement. Results showed more shrinkage, less stress relaxation, and higher restraint stress from the inclusion of metakaolin, potentially increasing cracking sensitivity of mixtures.

[1] This section was published in Construction and Building Materials[57]. Permission is included in Appendix A

CHAPTER 1: INTRODUCTION

Implementing supplementary cementitious materials (SCM) in concrete can provide an array of effects to improve its functionality. Factors such as compressive strength, modulus of elasticity, permeability, time of set and both shrinkage and expansion rates are altered through the use of SCMs. The main materials that have been used in recent years are fly ash, silica fume and slag. These constituents are given an additional title known as pozzolans because when they come in contact with water they undergo a pozzolanic reaction. A pozzolanic reaction is when the amorphous aluminosilicates of a pozzolan react with calcium hydroxide to produce calcium silicate hydrate[1].

Government agencies such as the Florida Department of Transportation (FDOT) have prescribed both upper and lower replacement limits of these materials based on the location and demands of the project to meet durability and strength requirements [2]. Although there are many positive factors from incorporating supplementary cementitious materials, there can also be consequences. Slag can improve long term strength, but it also can cause retardation by reducing not only the setting times but also the initial strength of the concrete. Although silica fume performs better with strength testing at all ages, it has penalties such as high heat release and increased shrinkage rates which has been shown to promote cracking.

A comparatively new cementitious material that has recently gained acceptance in construction practices and structural concrete applications is metakaolin. This material is known for its role in improving compressive strength and reducing the porosity of the concrete. Unlike

fly ash which is residue from coal burning power plants or silica fume which is made indirectly through manufacturing of silicon metal, metakaolin is not a byproduct and for this reason is substantially more expensive [1]. Metakaolin promotes stronger concrete through its high fineness and alumina content accelerating the hydration reaction, in addition to refining the pore structure. Working with metakaolin can be challenging due to its high fineness which requires a higher water demand, which can only be offset through increasing the water to binder ratio or increasing the dosages of chemical admixtures to increase workability. Metakaolin has been shown to produce similar results to that of silica fume in that it improves the higher early strength and permeability. Metakaolin also shares qualities ascribed to silica fume such as a higher heat release and increased shrinkage rates, while also decreasing the amount of creep generated [3], [4]. These drawbacks can severely heighten the probability of cracking in concrete structures incorporating these materials.

The focus of the current research is to determine how the incorporation of metakaolin influences the cracking potential of restrained concrete and to develop an understanding to the mechanisms responsible for the assessed behavior. Although testing has been performed on metakaolin to assess its shrinkage, there has been no testing in a rigid cracking frame (RCF) to determine metakaolin concrete performance under restrain and temperature profiles simulating massive structural elements. The rigid cracking frame testing is utilized to evaluate the developing uniaxial stress under an imposed temperature profile simulating the temperature of a 1 m^3 concrete element, which better relates to concrete being placed in the field than previous testing. In addition, this study shows the effect of temperature on the development of the hydration phases and pore structure in portland cement and portland cement-metakaolin concrete.

To satisfy a full investigation, the heat of hydration for the metakaolin paste sample was measured using isothermal calorimetry to determine the heat based activation energy of the mix. The determined activation energy was then used with semi-adiabatic calorimetry measurements to calculate the adiabatic temperature rise and hydration parameters for the studied systems. The temperature profile for the concrete mixtures was then developed and imposed in subsequent testing in the rigid cracking frame and the free shrinkage frame. Cracking potential was tested with a rigid cracking frame to apply restraint stresses during the initial 5 days of curing with the temperature profiled imposed. A free shrinkage frame under the same conditions was used to compliment the RCF data by determining the expansion and contraction of the concrete during its hydration after final set. Match cured cylinders were tested at several ages to monitor both compressive and tensile strengths, alongside with modulus of elasticity. In order to explain the stress development in the plain and blended concrete mixtures, pore size distribution studies using nitrogen adsorption and phase transformation studies using quantitative x-ray diffraction were subsequently conducted. The findings indicate that metakaolin has higher cracking potential in the system studied here due to phase transformation occurring at high temperatures that were accompanied by higher porosity in the microstructure of the cementitious paste.

CHAPTER 2: CRACKING POTENTIAL AND TEMPERATURE SENSITIVITY OF METAKAOLIN CONCRETE[2]

2.1 Abstract

Metakaolin is a pozzolanic material with the potential to reduce permeability and chloride ingress; however, quantification of the effects of metakaolin use on the cracking sensitivity of concrete mixtures is needed to ensure that these improvements in performance are not compromised. This study was conducted to investigate the early age cracking potential due to restraint stresses from incorporating metakaolin in concrete. Calorimetry testing showed that metakaolin was more sensitive to temperature than mixtures with only Portland cement. Results showed more shrinkage, less stress relaxation, and higher restraint stress from the inclusion of metakaolin, potentially increasing cracking sensitivity of mixtures.

2.2 Introduction

Concerns over the role of concrete constituent materials on early-age cracking susceptibility have led to research efforts to quantify these effects. Reductions in volume associated with thermal and autogenous shrinkage are the principal driving forces that lead to cracking. As the water-cementitious materials ratio (w/cm) decreases, cracking tendency increases because of higher amounts of autogenous shrinkage. As the amount of water present in the system decreases during hydration, low relative humidity conditions develop in the pores. These low-pressure pockets create tensile stresses on the pore walls as the water migrates through the system.

[2] This chapter was published in Construction and Building Materials[57]. The numbering has been modified from the published version to match the other chapters. Permission is included in Appendix A

This phenomena is attributed to the meniscus of the water becoming more narrow as the water tries to relocate within the pore network, causing the walls of the pores to pull closer together [5].

To meet durability standards, supplementary cementitious materials (SCMs) are now commonly included in concrete mixes. Materials such as slag, fly ash and silica fume have years of research and structural applications to identify the advantages and consequences of using these SCMs. Metakaolin is a newer SCM that is not being used as commonly in the field despite its benefit of high early strength and lower permeability.

These benefits are the result of the high lime consumption when metakaolin reacts with the hydrating paste and the paste undergoing a process called pore size refinement. This pore size refinement is an occurrence when the porosity of the paste decreases and the size of the pores are reduced. Although this process is useful in reducing chloride penetrability [6][7] and susceptibility to sulfates [8], this alteration in the microstructure of the paste has been shown to impact volume changes such as shrinkage and stress relaxation. It was found that increasing dosages of metakaolin will have positive correlation with free shrinkage rates[9]. Additionally, research on restraint stresses has been conducted on metakaolin but only at a constant temperature through ring testing without restraint on the outer edge of the concrete ring [9]. However, no research has been performed to test concrete with metakaolin for cracking potential when restrained under uniaxial conditions or how a predetermined temperature profile simulating semi-adiabatic conditions affects mechanical properties development, shrinkage, phase transformation and pore structure.

The overall research goal for this paper was to determine if any changes to early-age concrete behavior that affects cracking occur in concrete when metakaolin is added, the cause of any potential changes, and if this behavior precludes the use of the modified B3 model to simulate the early-age stress relaxation. In this study, rigid cracking frame tests were performed with a

predetermined temperature profile to provide means for measuring uniaxial stress development with concrete being exposed to temperatures comparable to that of a 1 m^3 concrete element. This stress development was investigated using isothermal calorimetry and semi-adiabatic testing to determine the heat sensitivity of the metakaolin mixture, while also using a free shrinkage frame and the testing of cylinders to track the development of shrinkage and mechanical properties when subjected to the same temperature profile, [10]. Pore size distribution characterization was performed using nitrogen adsorption and x-ray diffraction was also conducted to examine potential phase transformation that could affect the mechanical properties and stress development.

2.3 Materials and Methods

2.3.1 As-Received Materials Characterization

A Type I/II Portland cement and commercial metakaolin were used in this study. The as-received materials were characterized for their chemical, mineralogical and physical properties. The chemical oxide composition of the cement and metakaolin was determined by a certified external laboratory. Mineralogical characterization of the as-received materials as well as the hydrated cement-metakaolin paste was determined using a Panalytical X'Pert PW3040 Pro diffractometer coupled with Panalytical HighScore Plus software 3.1. The pattern was collected using Cu Kα radiation at a current of 40 mA and voltage of 45 kV; the step size was 0.02 degrees per step and counting time 4 seconds per step. Back-loading technique was used in placing the powder in the sample holder to minimize preferred orientation. The procedures of ASTM C1365 [11] were used in preparation of the powder for crystalline phases quantification. Blaine fineness was determined according to ASTM C204-11 [12] following instrument calibration using SRM 114q supplied by NIST. The specific gravity measurements were conducted in accordance to ASTM C188-09 [13].

Metakaolin was used at a 10% replacement level by mass. The concrete proportions for the control (CN) and metakaolin (10MK) mixtures used in free shrinkage, mechanical properties and cracking frame tests are presented in Table 1.

Table 1. Mix design for concrete ($1m^3$)

Material	CN	10MK
Cement (kg/m^3)	445	400
Metakaolin (kg/m^3)	0	44
Coarse Aggregate (saturated surface dry) (kg/m^3)	949	949
Fine aggregate (saturated surface dry) (kg/m^3)	624	607
Water (kg/m^3)	154	154
Air entraining admixture (mL/100kg cementitious)	7	7
Type A/F admixture (mL/100kg cementitious)	390	390
Type D admixture (mL/100kg cementitious)	304	304
w/cm ratio	0.35	0.35

A w/cm ratio of 0.35 was maintained constant by adjusting the mix water for the water content of the chemical admixtures. The same proportions of the cementitious constituents were maintained in paste mixtures for isothermal calorimetry, nitrogen adsorption and x-ray diffraction experiments.

2.3.2 Isothermal Calorimetry

In assessing the effect of metakaolin on the hydration kinetics and temperature sensitivity of the cementitious mixtures, isothermal calorimetry was performed on 10MK paste samples using a TAMAIR eight-channel isothermal conduction calorimeter. Tests were conducted at three different temperatures (23, 30 and 40 ºC). The w/cm ratio was maintained at 0.35 and included

chemical admixtures at the same proportions adopted for the corresponding concrete mixtures. The test was conducted in accordance to ASTM C1702 [14] Procedure B for external mixing. The cumulative heat of hydration at the three temperatures was then used to calculate the mixture activation energy using the procedure outlined by Poole et al.[15]. The activation energy was determined following Equation 1:

$$\alpha\,(t_e) = \alpha_u \cdot \exp\left(-\left(\frac{\tau}{t_e}\right)^{\beta}\right) \qquad \text{Equation 1}$$

where, α (t) = Degree of hydration at age t,

α_u = Ultimate degree of hydration,

τ = Time parameter (hours),

β = Shape parameter, dimensionless, and

t = Elapsed time since the contact of cementitious material and water (hours)

In this procedure, the α_u, β, and τ parameters were fit so that the degree of hydration with time fit to that calculated from the cumulative isothermal calorimetry heat of hydration results at 23°C. The degree of hydration was calculated from isothermal calorimetry results using Equations 2 through 4:

$$\alpha(t) = \frac{H(t)}{H_u} \qquad \text{Equation 2}$$

$$H_u = H_{cem} \cdot p_{cem} + 461 \cdot p_{slag} + 1800 \times p_{FA-CaO} \cdot p_{FA} + 330 p_{SF} \qquad \text{Equation 3}$$

$$H_{cem} = 500 \cdot p_{C_3s} + 260 \cdot p_{C_2S} + 866 \cdot p_{C_3A} + 420 \cdot p_{C_4AF} + 624 \cdot p_{SO_3} + 1186 \cdot p_{FreeCa} + 850 \cdot p_{MgO} \quad \text{Equation 4}$$

where H(t) is the cumulative heat of hydration by mass of cement (J/g) from isothermal calorimetry at time t, p_{cem} is the % of cement by mass in the cementitious system, p_{slag} is the % of slag cement by mass in cementitious system, $p_{FA\text{-}CaO}$ is the % CaO in the fly ash used, p_{FA} is the % of fly ash by mass in cementitious system, p_{SF} is the % of silica fume by mass in cementitious system, p_i is the % of *i*th component by mass in cement. Since the ultimate heat of hydration contribution from metakaolin is not known, the value for silica fume was used in the analysis. Errors in H_u could cause a change in the calculated α_u fit parameter, but will not change the overall calculated adiabatic temperature development.

After the parameters were fit to the cumulative heat of hydration results at 23°C, the τ parameter was fit to the cumulative isothermal calorimetry heat of hydration results at the 30°C and 40°C temperatures using the α_u and β parameters fit at 23°C. The τ values from each temperature were then used as the rate constants in an Arrhenius plot to calculate the apparent activation energy.

2.3.3 Semi-Adiabatic Calorimetry

Semi-adiabatic calorimeters contain a heavily insulated concrete sample. This system allows a slight amount of heat to escape the enclosed system. Sensors in the calorimeter measure the heat loss rate in the calorimeter with time. The sensors in the calorimeter were calibrated by monitoring the heat loss rate with time using hot water placed in the calorimeter. The measured concrete sample temperature development and heat loss with time was then used to calculate the temperature rise, simulating an adiabatic system [15]. Measurements for semi-adiabatic

calorimetry were conducted using instruments assembled at the University of South Florida. Obtaining the adiabatic temperature rise of concrete is a multistep process that involves determining the heat based activation energy of concrete mixture through isothermal calorimetry, calibration of the semi-adiabatic calorimeter and assessment of temperature loss, measurements of concrete temperature development in the semi-adiabatic calorimeter and calculating the fully adiabatic temperature rise. The fully adiabatic temperature rise was fit from the measured concrete temperature development and heat loss following the procedures recommended by RILEM [16]. The heat of hydration curve used in the fitting followed Equation 5 [17].

$$Q_h(t) = H_u \cdot C_c \cdot \left(\frac{\tau}{t_e}\right)^{\beta} \cdot \left(\frac{\beta}{t_e}\right) \cdot \alpha_u \cdot exp\left(-\left[\frac{\tau}{t_e}\right]^{\beta}\right) \cdot \exp\left(\frac{E_a}{R}\left(\frac{1}{T_r}+\frac{1}{T_c}\right)\right) \quad \text{Equation 5}$$

where $Q_h(t)$ is the rate of heat release with time t, H_u is the total heat available for reaction (J/g), C_c is the cement content (kg/m^3), α_u, τ, and β are hydration coefficients, t_e is the concrete equivalent age maturity, E_a is the activation energy calculated from isothermal calorimetry, R is the universal gas constant, T_r is the concrete reference temperature taken to be 296.15 °K, and T_c is the concrete temperature at time t (°K). H_u can be calculated from the cement composition as shown in Equations 3 [18] and 4 [17].

2.3.4 Concrete Temperature Profile

The temperature profile used in the testing simulates the temperatures that would be exhibited in a concrete mass element. In order to make the predetermined temperature profile, the temperature at the center of a newly placed concrete wall 1.0 m thick with a constant surface temperature was simulated using the experimental data collected from the semi-adiabatic calorimetry [19].

2.3.5 Time of Set

Mineral admixtures and chemical admixtures can play an extensive role on the initial and final set of concrete. To determine the time of set for each mix, ASTM C403 [20] penetration test was conducted on mortar sieved from each concrete mixture. The data was then used to determine when to back off the plates for the free shrinkage measurements in order to release any restraint provided on the specimen ends. The mortar was cured under simulated conditions that matched the temperature profile used for the cracking frame and free shrinkage tests.

2.3.6 Mechanical Properties

Twenty 100 mm x 200 mm concrete cylinders were matched cured according to the same temperature profile used in the rigid cracking frame and free shrinkage frame to evaluate the mechanical properties of 10MK and CN mixtures. The parameters that were investigated using the concrete cylinders were: compressive strength, splitting tensile strength and elastic modulus at the ages of 12 h, 1 day, 3 days and 7 days. At the 4-day age, the cylinders were removed from the temperature regulated water bath and placed in room temperature water. These tests were conducted in accordance to ASTM C39 [21], ASTM496 [22] and ASTM469 [23], respectively. All cylinders were demolded at the time of testing and variances in measured data were within limits specified in the corresponding specifications.

2.3.7 Free Shrinkage

To quantify the linear strain developed by concrete, a free shrinkage frame [20] was used, Figure 1, based on the design adopted from Meadow [24]. The frame has copper pipes built into the formwork to control the temperature of the concrete by using temperature-regulated water that follows the modeled temperature. Two sheets of plastic were sprayed with a lubricant and used to line the formwork to minimize friction. Two moveable end plates were present in the free

shrinkage frame to keep the concrete restrained until final set occurred. Once final set was reached, the plates were retracted to allow the concrete to expand, uninhibited, in the longitudinal direction. Loss of moisture was eliminated during the test, to avoid drying shrinkage, by sealing the concrete in plastic and waterproof tape. The concrete specimen length change was monitored by two LCP sensors attached to 3 mm diameter invar rods. The invar rods were attached to 25 mm square aluminum plates embedded in the concrete samples.

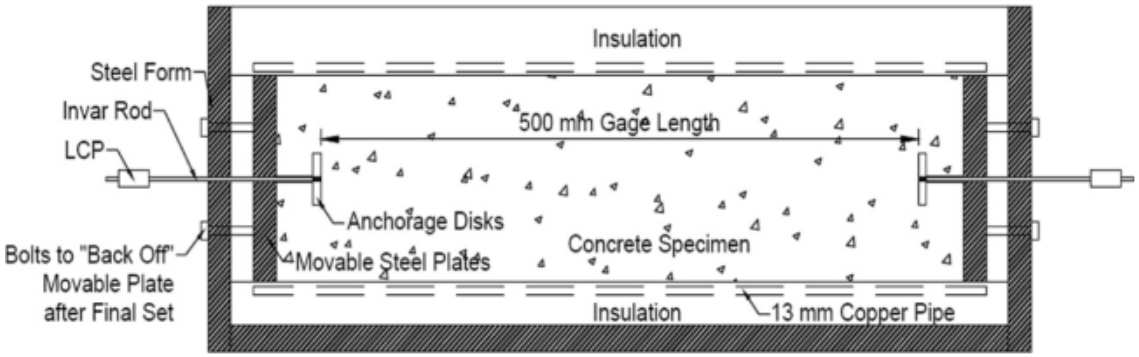

Figure 1. Free shrinkage frame [25]

2.3.8 Rigid Cracking Frame

The rigid cracking frame allows comparison of the early-age cracking sensitivity and quantification of stress relaxation properties during the hardening stage of concrete mixtures [26]. In this test, a dove-tailed concrete specimen was placed in the frame shown in Figure 2 and allowed to harden. This frame is based on the original design by Springenschmid, with slight modification for the cross-sectional area for the concrete while maintaining the same concrete cross-sectional area to the invar bars cross-sectional area [27]. The frame contains two invar steel bars that restrained the concrete from changing length. The concrete temperature was controlled to the predetermined temperature profile by circulating tempered water through the frame crossheads and copper pipes embedded in the formwork. As the concrete heated up, the frame restrained the

concrete from expanding, causing the concrete to go into compression and the invar steel bars to go into tension. As the concrete stress relaxed, and the concrete began to shrink due to thermal or autogenous shrinkage, the concrete went into tension while the invar steel bars went into compression. The rigid cracking frame used in this study contained a concrete specimen with a center cross section of 100x100 mm and 1041mm in length [25].

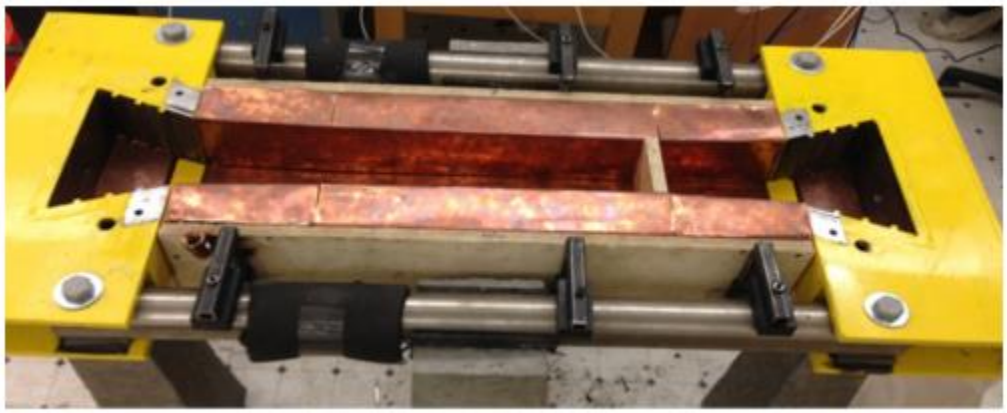

Figure 2. Rigid cracking frame[20]

The concrete degree of restraint changed with time and was a function of the rigid cracking frame stiffness, concrete cross section area and modulus of elasticity as shown in Equation 6, [28].

$$\delta = \frac{100}{1 + \frac{E_c A_c}{E_s A_s}} \qquad \text{Equation 6}$$

where δ is the concrete degree of restraint, E_c is the concrete modulus of elasticity (MPa), A_c is the concrete cross sectional area (m^2), E_s is the invar steel modulus of elasticity (MPa), and A_s is the invar steel cross sectional area (m^2).

The concrete creep parameters were calculated using the modified B3 model. The original B3 model was developed by Bažant and Baweja to model the effects of creep on concrete after 1

day of age [29]. The B3 model was modified to account for early-age viscoelastic response before one day by modifying the q_1 and the q_2 term in the model in Equations 7 through 10 to give Equation 11, [30].

$$q_1 = \frac{0.6}{E_{c,28}} \quad \text{Equation 7}$$

$$q_2 = (86.814)(10^{-6})(c^{0.5})(f_{c,28}^{-0.9}) \quad \text{Equation 8}$$

$$q_3 = 0.29(w/c)^4 q_2 \quad \text{Equation 9}$$

$$q_4 = (0.14)(10^{-6})(a/c)^{0.7} \quad \text{Equation 10}$$

$$J(t,t_0) = q_1\left[\frac{t_0}{t_0 - q_6}\right] + q_2\left[\frac{t_0}{t_0 - q_5}\right]Q(t,t_0) + q_3\ln(1 + (t - t_0)^n) + q_4\left(\frac{t}{t_0}\right) \quad \text{Equation 11}$$

where $J(t,t_0)$ is the creep compliance at time t from loading at time t_0, $E_{c,28}$ is the concrete elastic modulus at 28 days (psi), q_5 and q_6 are early-age modification terms that should not exceed the setting time (days), c is the cement content (lb/yd^3), a is the total aggregate content (lb/yd^3), w/c is the water-cement ratio by mass, n equals 0.1, and m equals 0.5. The principle of superposition was used to model the stress relaxation development with time [31]. In this study, the water-cementitious materials ratio (w/cm) was used since one of the mixtures contained supplementary cementitious materials. The cracking frame stress modeled using the measured elastic modulus, free shrinkage, and modified B3 model were compared against the measured cracking frame stress for the mixtures.

2.4 Results and Discussion

2.4.1 As-Received Materials

The elemental oxide composition and the physical characteristics of the as-received materials are presented in Table 2. The crystalline phase content of the as-received materials are presented in Table 3. The results indicate the presence of 3 forms of calcium sulfates in the as-received cement; namely, anhydrite, hemihydrate and gypsum. No double salts were identified. The amount of tricalcium aluminate is higher than that calculated through Bogue equations and only the cubic structure is noted. As for metakaolin, the amount of crystalline phases present did not exceed 2% indicating a high potential pozzolanic activity for the metakaolin used here.

Table 2. Chemical composition and physical properties of as-received materials

Analyte	Portland Cement (w/o)	Metakaolin (w/o)
SiO_2	20.4	51.29
Al_2O_3	5.2	44.16
Fe_2O_3	3.2	0.49
CaO	63.1	<0.01
MgO	0.8	0.14
SO_3	3.6	<0.01
Na_2O	0.1	0.26
K_2O	0.38	0.27
TiO_2	0.28	1.12
P_2O_5	0.12	0.06

Table 2 (Continued)

Mn_2O_3	0.03	<0.01
SrO	0.08	0.01
Cr_2O_3	0.01	0.01
ZnO	<0.01	<0.01
L.O.I. (950°C)	2.8	1.4
Total	100.1	99.22
Na_2O_{eq}	0.35	0.44
Free CaO	2.23	N/A
BaO	N/A	<0.01
Specific Gravity	3.14	2.23
Blaine Fineness(m^2/kg)	442	N/A

Table 3. Mineralogical composition of as-received materials

Phase	Amount (%)
Type I/II Portland Cement	
C_3S	46.9
C_2S	25.2
C_3A (cubic)	9.6
C_4AF	8
Gypsum	2.8
Hemihydrate	1.8

Table 3 (Continued)

Anhydrite	0.5
Calcite	2
Portlandite	2.5
Quartz	0.8
Metakaolin (MK)	
Mullite	1
Illite	0.7
Quartz	0.3

2.4.2 Isothermal Calorimetry

Figure 3 shows the heat flow curves for the control (CN) and metakaolin (10MK) pastes at 23ºC. Since external mixing was used here, the first peak, reflecting ionic dissolution was not registered. The increased rate of heat flow noted on the inclusion of metakaolin and its accelerating effect on the hydration kinetics can be attributed to both its amorphous content and high surface area, [32] [33]. The effects of including metakaolin result in a shift in the silicate peak position from about 8 hours for CN paste to 4 hours in 10MK paste. The main hydration peak magnitude also increased when metakaolin was used. The noted increase indicates the significance of metakaolin on the hydration process of cement and the effect can be attributed to enhancing the hydration kinetics through heterogeneous nucleation. The effect of metakaolin extends to the sulfate depletion peak [34], which shows substantially higher magnitude, indicating the significance of incorporating metakaolin on hydration reaction of tricalcium aluminate and ettringite formation [35].

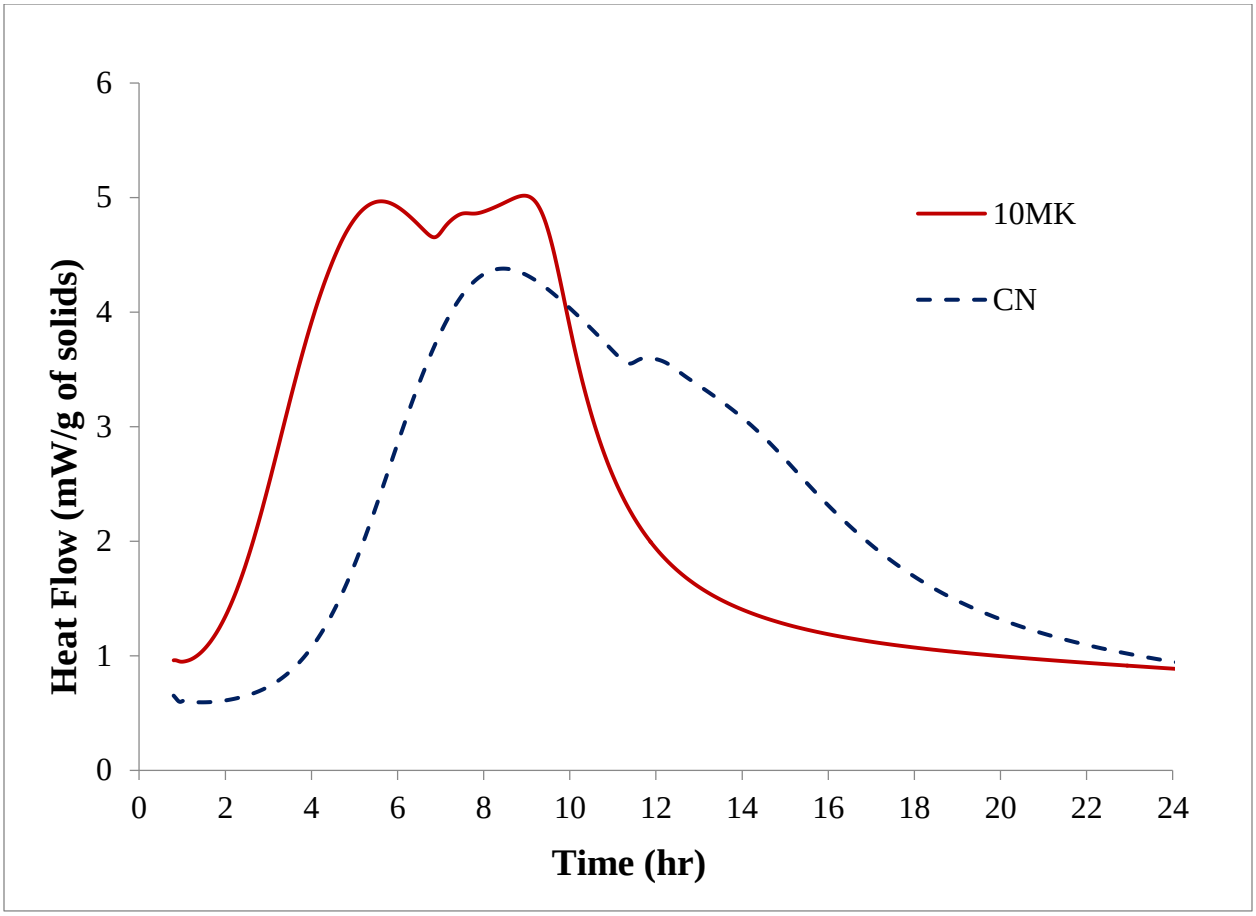

Figure 3. Isothermal heat flow profiles for 10MK and CN at 23° C

These trends are amplified with increasing temperature as can be seen from Figure 4. The silicate peak associated with C_3S hydration shifts towards shorter times with increasing temperature indicating the effectiveness of metakaolin on enhancing or accelerating the silicate reaction [36]. The effect of metakaolin is also significant on the hydration reaction of C_3A. Figure 4 shows that incorporation of metakaolin results in increasing the rate of heat flow for the sulfate depletion peak by a factor of 4 as temperature increased from 23 to 40ºC. The substantial increase in the hydration reaction of the aluminate peak could be due to the effect of temperature on enhancing the reactivity of the aluminates [37], decreasing sulfates availability [38] or a combination of both.

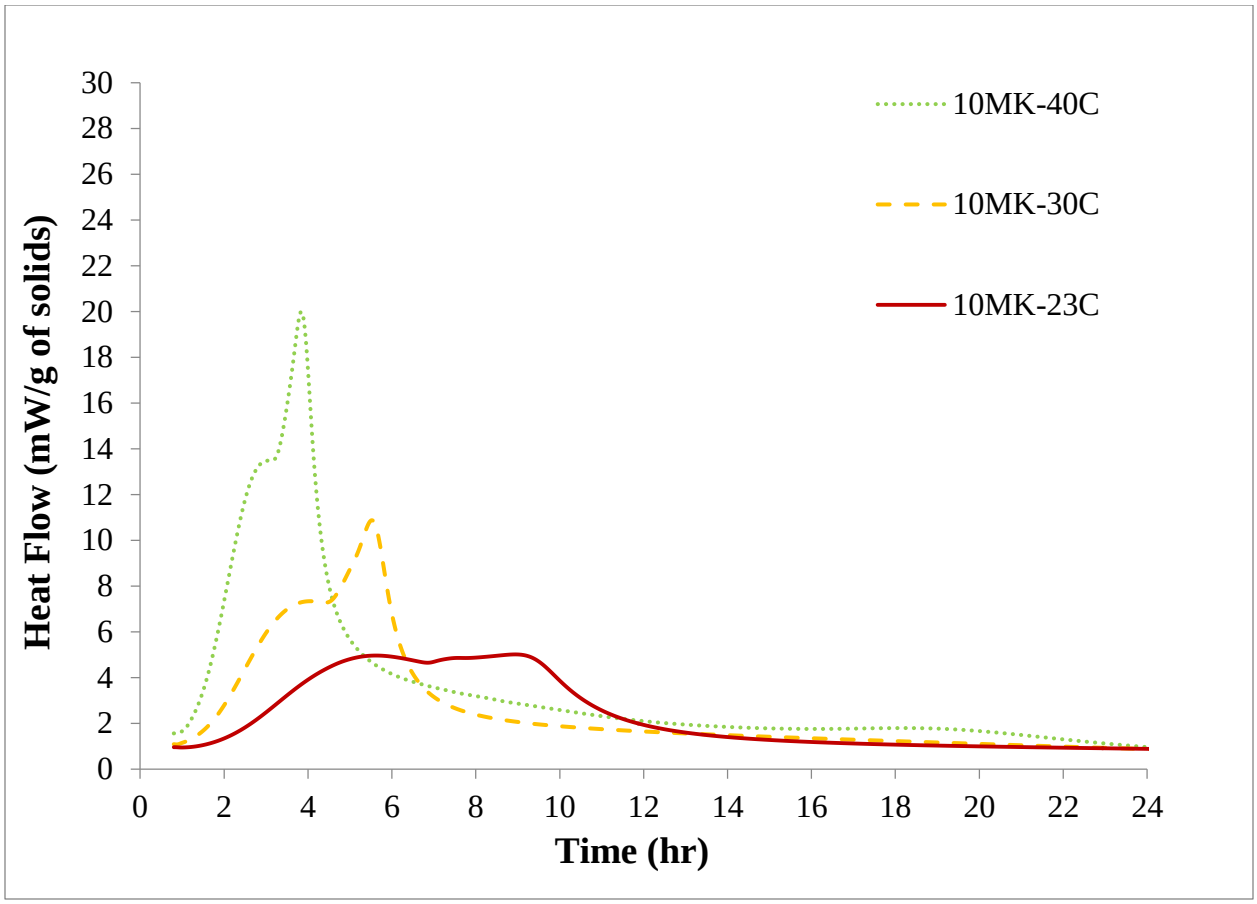

Figure 4. Isothermal heat flow profiles for 10MK at 23, 30 and 40 °C

The adjustment in the heat flow with increasing the dosage of metakaolin beyond 10% replacement to 21% can be seen in Figure 5. Although at 23ºC the sulfate depletion point is more prominent than both 10MK and CN, the location of this point does not shift when compared to 10MK. At 40ºC the effects of higher metakaolin dosage are most notable with the sulfate depletion point being shifted approximately an hour earlier than 10MK and having a 25% increase in heat flow. The temperature sensitivity of metakaolin can also be distinguished with the 21MK having a heat based activation energy of 45 (kJ/mol), while the control was at 36 (kJ/mol).

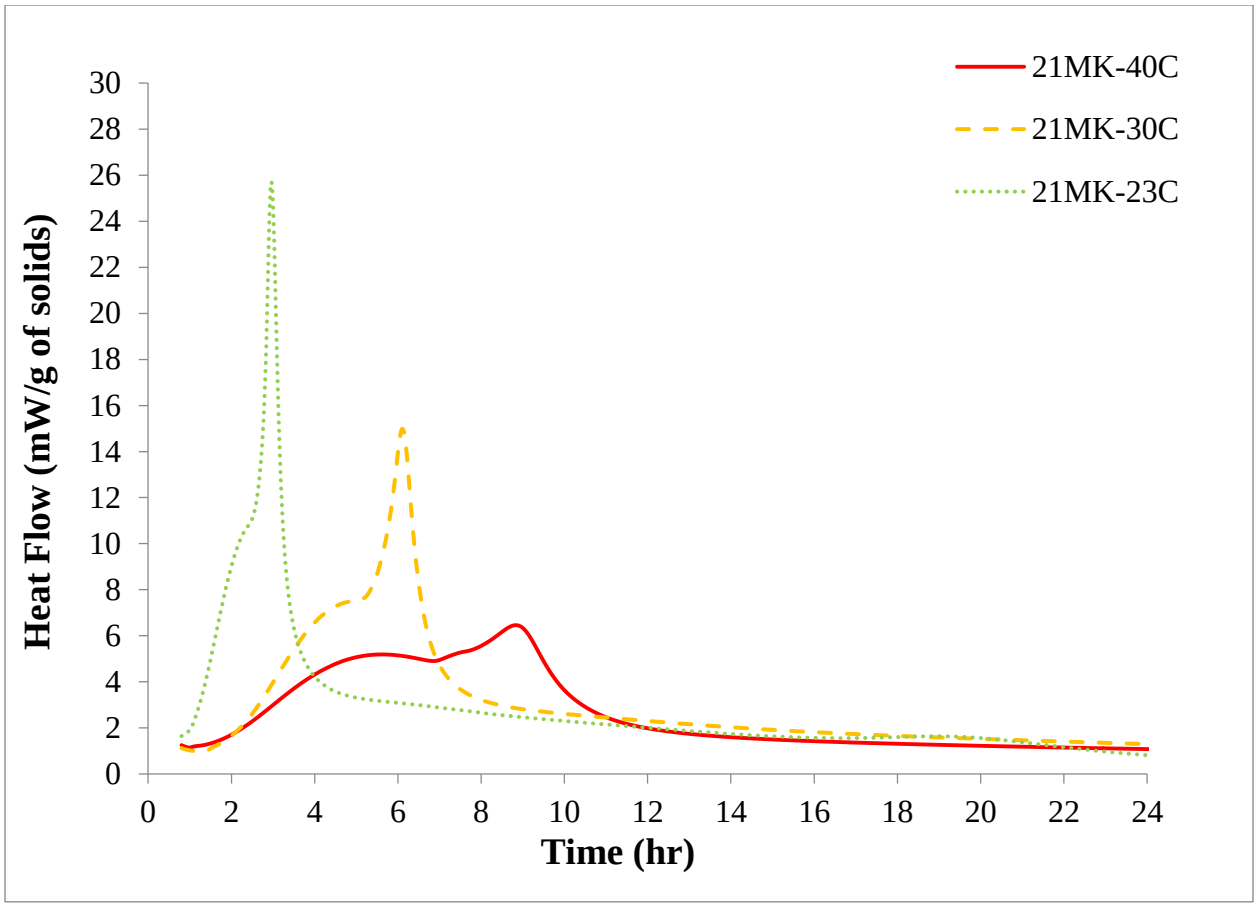

Figure 5. Isothermal heat flow profiles for 21MK at 23, 30 and 40 °C

2.4.3 Semi-Adiabatic Calorimetry

Concrete mixture proportions for CN and 10MK are depicted in Table 1. Semi-adiabatic measurements for 10MK concrete showed higher heat of hydration than CN as shown in Figure 6, which correlates well with isothermal-calorimetry measurements. Table 4 shows the mixture adiabatic heat rise parameters calculated from semi-adiabatic calorimetry and activation energy calculated from the isothermal calorimetry.

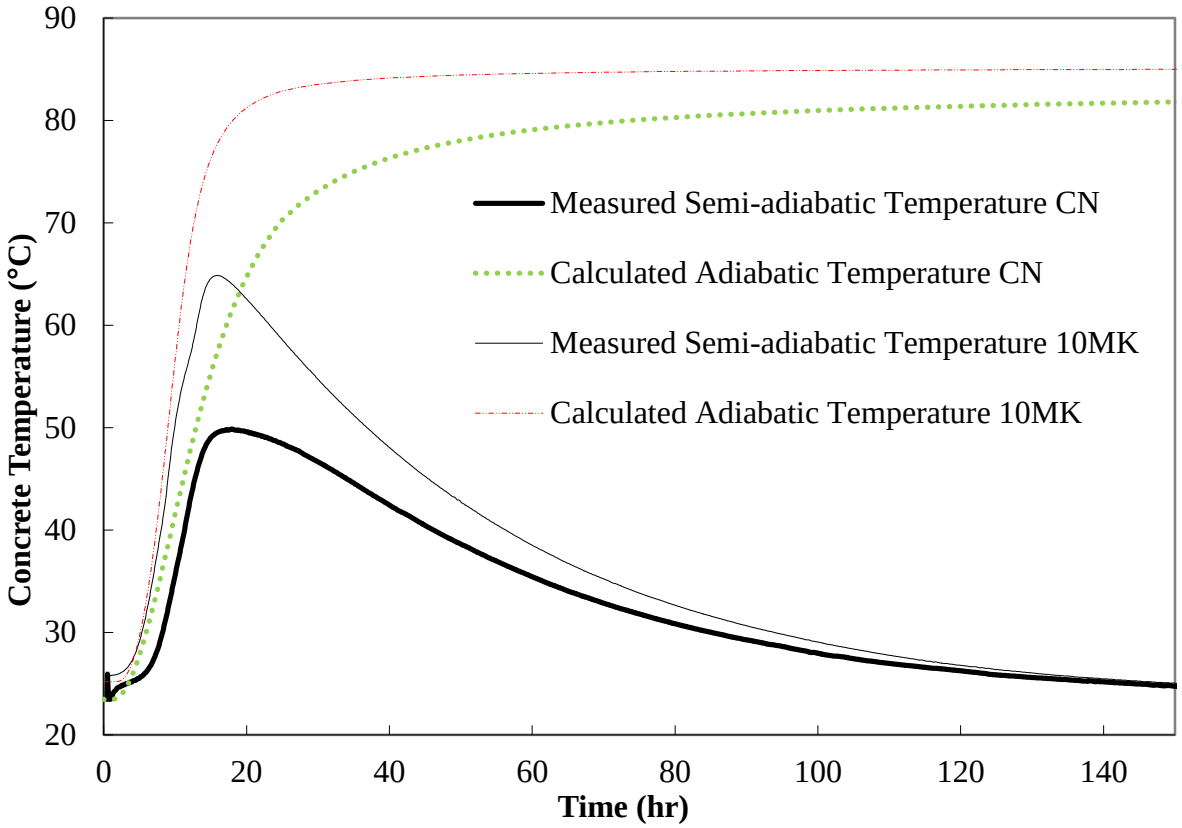

Figure 6. Semi-adiabatic calorimetry results for 10MK and CN

Table 4. Calculated concrete hydration parameters from isothermal calorimetry (Ea) and semi-adiabatic calorimetry (α_u, β, τ)

Hydration Parameters	CN	10MK
α_u	0.738	0.727
β	0.826	1.164
τ (hrs)	18.39	13.93
Ea (kJ/mol)	36	42.5

2.4.4 Concrete Temperature Profile

A custom-written temperature simulation and control program was used to generate an individual temperature profile for 10MK and CN. This temperature profile was used for the rigid cracking frame, free shrinkage and match curing specimens based on the temperature in a simulated 1 m thick wall [15], [35]. This program uses the mix design, heat-based activation energy, α_u, β, τ from semi-adiabatic testing and the ultimate heat of hydration as inputs. The heat-based activation energy for 10MK was determined from isothermal calorimetry tests at 3 temperatures; namely, 23, 30 and 40° C. The activation energy was calculated using an Arrhenius relationship [40] and shown in Table 4. Semi-adiabatic calorimetry data was collected and analyzed to determine the concrete hydration parameters α_u, β, τ by using the determined activation energy and the ultimate heat of hydration. A best-fit analysis was used to calculate the hydration parameters using an iterative process outlined by RILEM 119 [16]. To utilize the Rigid Cracking Frame Temperature Profile Program [41], the concrete thermal conductivity was estimated based on the mixture proportions and aggregate types in the analysis to be 2.70 W/m/°C, while the concrete specific heat was estimated to be 854.43 J/kg/°C. After 96 hours of curing, the concrete temperature profile was set to decrease at 1 °C/hr. Figure 7 shows the calculated concrete temperature profiles.

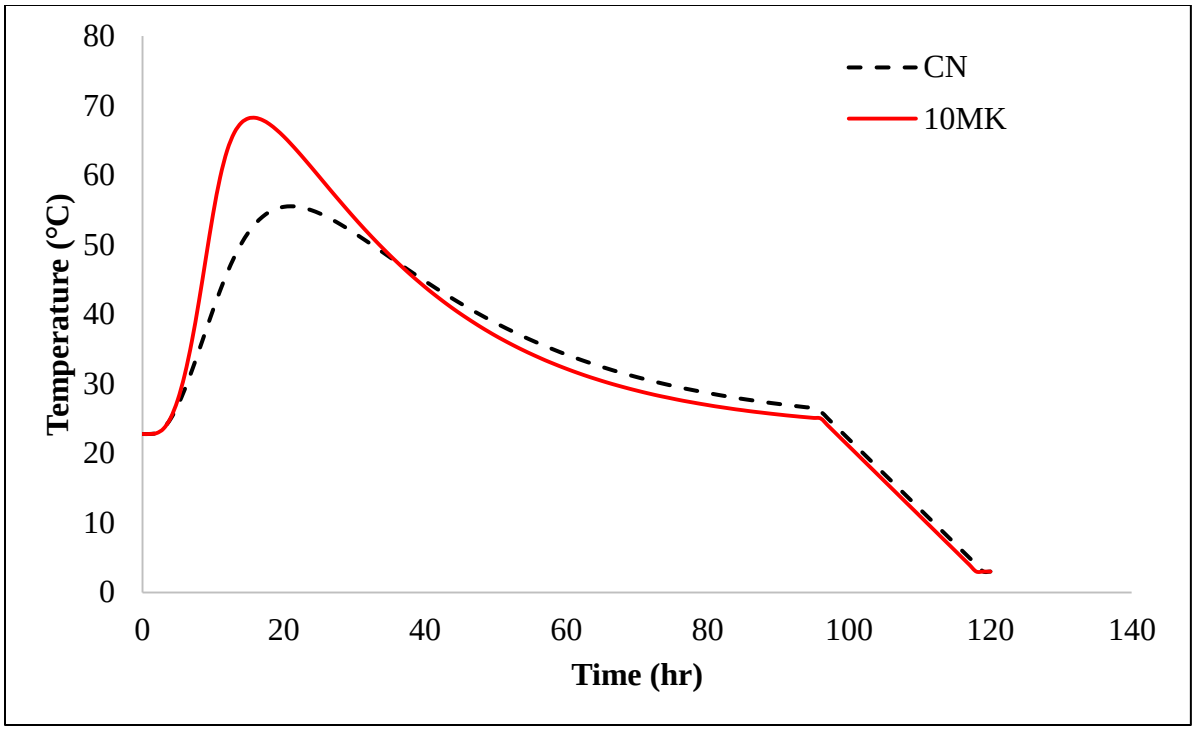

Figure 7. Temperature profiles of 10MK and CN

2.4.5 Mechanical Properties

The results for the compressive strength, splitting tensile strength and elastic modulus testing are presented in Table 5 through Table 7. The inclusion of metakaolin had a pronounced effect on the mechanical properties of concrete. The compressive strength observed in the earlier and later stages of testing for 10MK are consistently higher than CN. There are some conflicts in the literature that show varying results from the inclusion of metakaolin in regards to compressive strength. Some researchers have shown that using metakaolin increases compressive strength at both a w/cm of 0.25 and 0.35 at all ages beyond about 4 days [42]. This increase in compressive strength can be attributed to a denser structure and to better bonding between cement paste and aggregate particles [42].

Table 5. Concrete compressive strength

Age (Days)	CN (MPa)	10MK (MPa)
0.5	20.06	25.58
1	43.71	59.16
3	50.61	60.33
7	57.85	60.19

Table 6. Concrete splitting tensile strength

Time (Days)	CN (MPa)	10MK (MPa)
0.5	2.38	2.65
1	3.55	4.45
3	4.69	4.65
7	4.21	4.41

Table 7. Concrete elastic modulus

Age (Days)	CN (MPa)	10MK (MPa)
0.5	25.25	26.03
1	35.16	37.4
3	38.7	40.33
7	40.25	39.13

Other researchers have found that the pozzolanic reaction between metakaolin and calcium hydroxide, the acceleration of Portland cement hydration, and the filler effect have a large impact on the strength development when metakaolin is used [43]. Dinakar et al. found that with an

optimum replacement level of 10%, metakaolin yields higher compressive strength after the first few days of curing [44] . Other studies have found that 10% replacement is the optimal dosage at approximately 56 days, having an additional 2.7MPa over the control [41].

One interesting feature between the two mixes is the strength development after 1 day. 10MK showed almost no strength development, while the CN was still increasing at a modest rate. This difference in strength improvement rates can be attributed to the faster hydration of 10MK similar to the observed trends from isothermal calorimetry tests.

The splitting tensile strength development is almost identical between 10MK and CN but does not display the same strength gain trends noted for compressive strength development. 10MK gave consistently higher values at all testing ages considered here, with the 1 day strength defining significant differences. 5% and 15% replacement levels have shown to be effective in increasing the splitting tensile strength according to Güneyisi et al. [42]. A previous study has found 10% substitution to be most successful in increasing the splitting tensile strength [44]. Having dosages of replacement at and beyond 20% have shown reductions in strength when compared to the control, while 10-15% replacement is found to be the most optimal for improving splitting tensile strength [45].

Modulus of elasticity improved during the early stages of hydration with the inclusion of metakaolin. For both mixes, after one day of curing, the rate at which the modulus of elasticity increased appears lower. This rapid and then stagnant growth in the modulus of elasticity may be attributed to the modulus of elasticity development rate typically occuring faster than compressive strength development rate and the match curing effect on accelerating the hydration reaction.

2.4.6 Free Shrinkage

Free shrinkage measurements, shown in Figure 8, commenced after final set. Initial and final set measurements are presented in Table 8.

Table 8. Setting time for CN and 10MK

Property	CN (min)	10MK (min)
Initial set	358	218
Final set	434	311

Both concrete mixtures exhibited similar expansion rates for the first 12.5 hours. The switch from expansion to contraction for 10MK began at an earlier time and after less expansion has occurred. The higher rate of shrinkage that occurred in the 10MK can be attributed to autogenous shrinkage and thermal effects. The expansion occurring in the early stages of hydration can be attributed to the properties of the materials and the effect of temperature. The reaction between cementitious materials and water is an exothermic and expansive process. Temperature plays a role in this combination because higher temperatures increase the hydration reaction, which is one of the reasons that the 10MK went into shrinkage earlier than CN. The high heat generation that 10MK displayed can be credited to the high fineness associated with metakaolin [46], the very high consumption rate of lime by the metakaolin [47], and the higher heat of hydration associated with the aluminate phases compared to silicates.

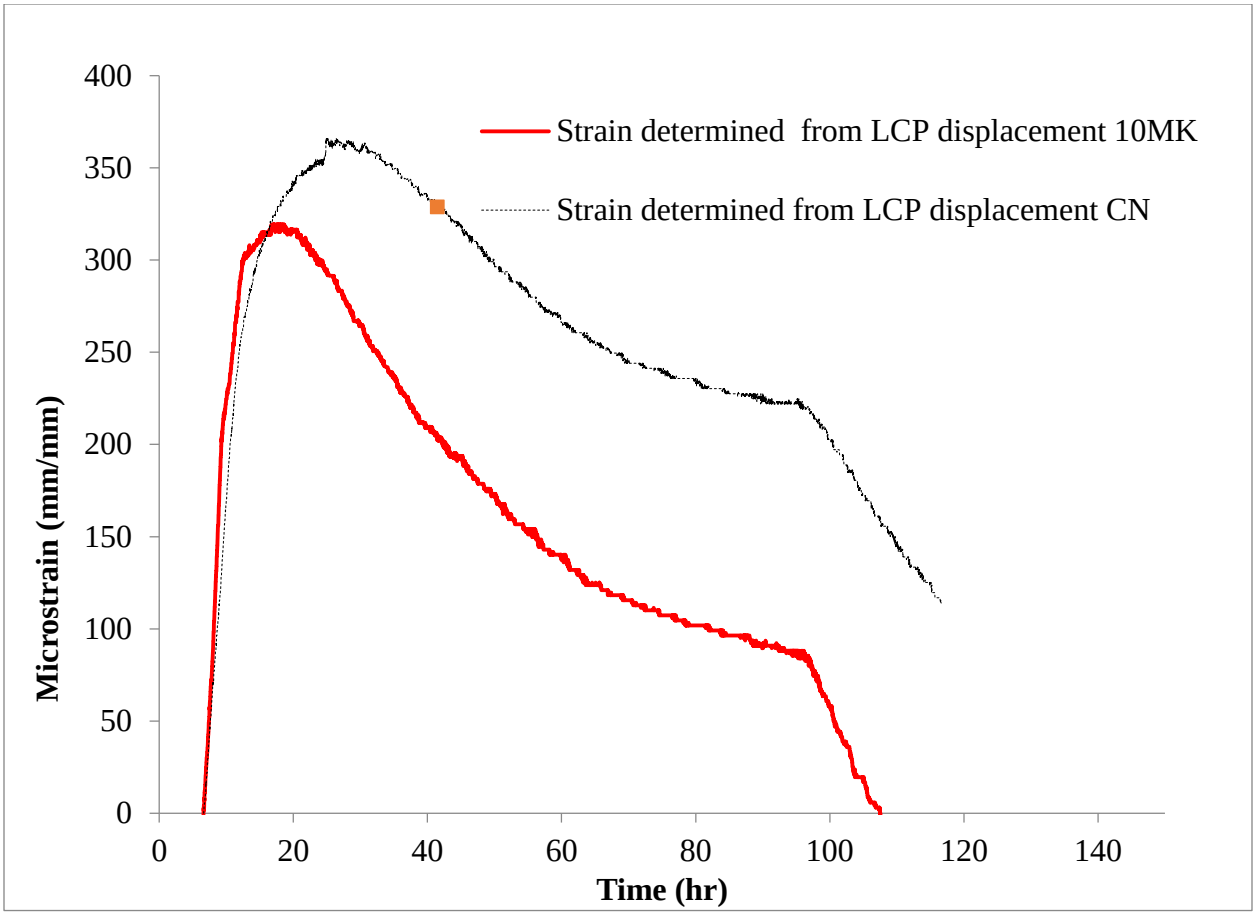

Figure 8. Free shrinkage strain for CN and 10MK concrete

One of the possible causes for the increased shrinkage rate associated with 10MK is the different microstructure development in MK concrete. Mercury intrusion porosimetery testing, performed by other researchers, showed that the cement paste microstructure undergoes pore size refinement and has a finer pore size distribution in MK pastes [48],[49]. These smaller pores yield consequences similar to those of including silica fume where higher stresses are imposed on the walls of the paste pores. The capillary pressure forces were likely higher than those generated in the CN mixture and were generated by the water meniscus being pushed farther out due to the refined pore structure and drawing the walls closer together, accounting for a higher overall shrinkage in 10MK. Other researchers showed that for replacement levels that are 10% or below,

the autogenous shrinkage is actually higher than for the control mixtures with only Portland cement [50]. More recent research has isolated the effects of autogenous shrinkage and have shown that low w/b mixtures will exhibit higher autogenous shrinkage up to 9 days depending on the replacement levels of metakaolin [51].

Limited x-ray diffraction study was also conducted on the 10MK paste after subjecting it to the same temperature profile as the 10MK concrete mixture. The data indicate decomposition of ettringite at temperatures above approximately 45ºC (8 hours) and formation of the lower sulfate hydrate forms; that is, monosulfoaluminates with variable water content (n=H_2O=14, 13, and 12). This phase decomposition is expected to be accompanied by a decrease in the solid volume [52]. The prevalence of this transformation is shown in the diffraction scans of the paste fraction of 10MK presented in Figure 9. Quantitative analyses using Rietveld refinement indicate a decrease in the mass fraction of ettringite by more than 60% at 16 hours (corresponding to the initiation of reversible of length change measurements from expansion to contraction) compared to its mass fraction at 8 hours. Lothenbach et al [53], using thermodynamic modelling and strength testing of cubes, associate this transformation with increase in paste porosity as monosulfoaluminates occupy half the molar volume of ettringite.

Harada and Matsushita [54], by varying gypsum content, attempted to reduce the autogenous shrinkage observed for low heat slag cement intended for massive structures when hydrating at temperature higher than 40°C. The increased autogenous shrinkage was attributed to the presence of higher alumina content in the pore solution of slag blends which accelerate the transition of ettringite to monosulfoaluminates [54]. Lura et al. [55] had previously attributed the higher autogenous shrinkage observed in slag cement, relative to modeled values accounting for capillary tension, to this phase transformation. XRD analysis conducted here confirms similar

phase transformation in metakaolin, which has higher alumina content than slag but is typically added at lower replacement levels in concrete mixes.

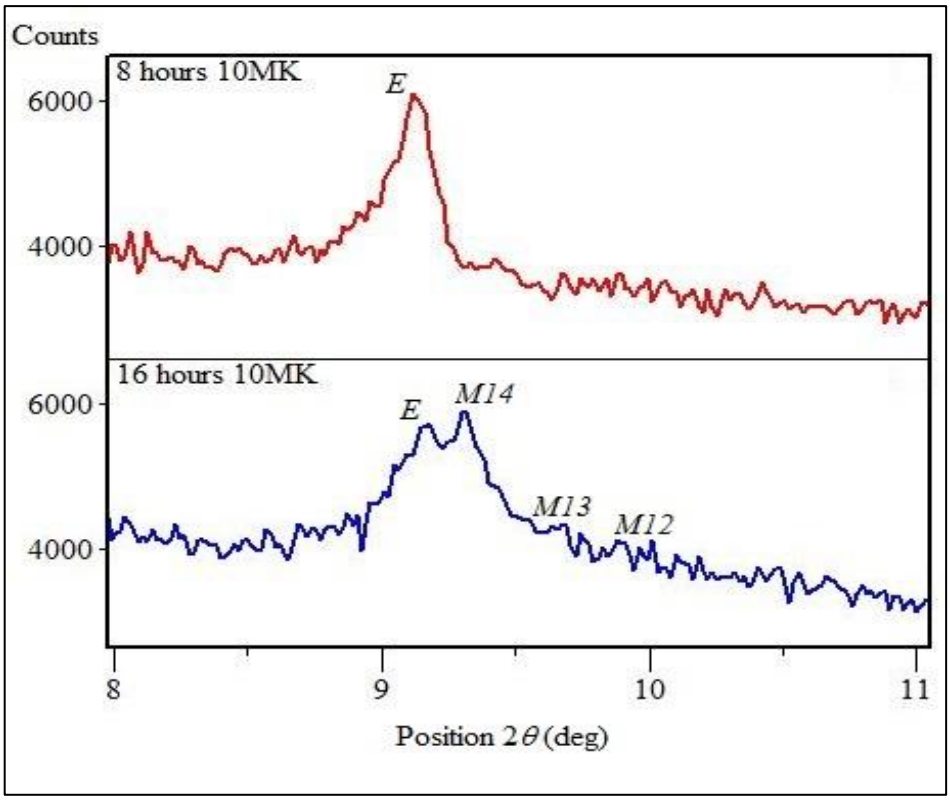

Figure 9: QXRD peak indicating phase transformation from Ettringite (Aft) to Monosulfoaluminates (AFm) between 8 and 16 hours (E – ettringite, M – monosulfoaluminates)

In order to assess if the identified phase transformation in 10MK mixture had an effect on pore size distribution, nitrogen adsorption tests (NAD) were conducted on 10MK paste samples prepared at hydration ages of 8 and 16 hours and exposed to the same temperature profile as the cracking frame, free shrinkage and XRD experiments. This hypothesis was confirmed here through the pore size distribution measurements shown in Figure 10. The data indicate pore size refinement and increase in pores in the pore size range of 3 to 100 nm at 16 hours when compared to 8 hours.

Though the degree of hydration at 8 and 16 hours were 0.196 and 0.622, respectively, the increase in porosity in the pore size range of 3-100 nm is more likely related to ettringite decomposition.

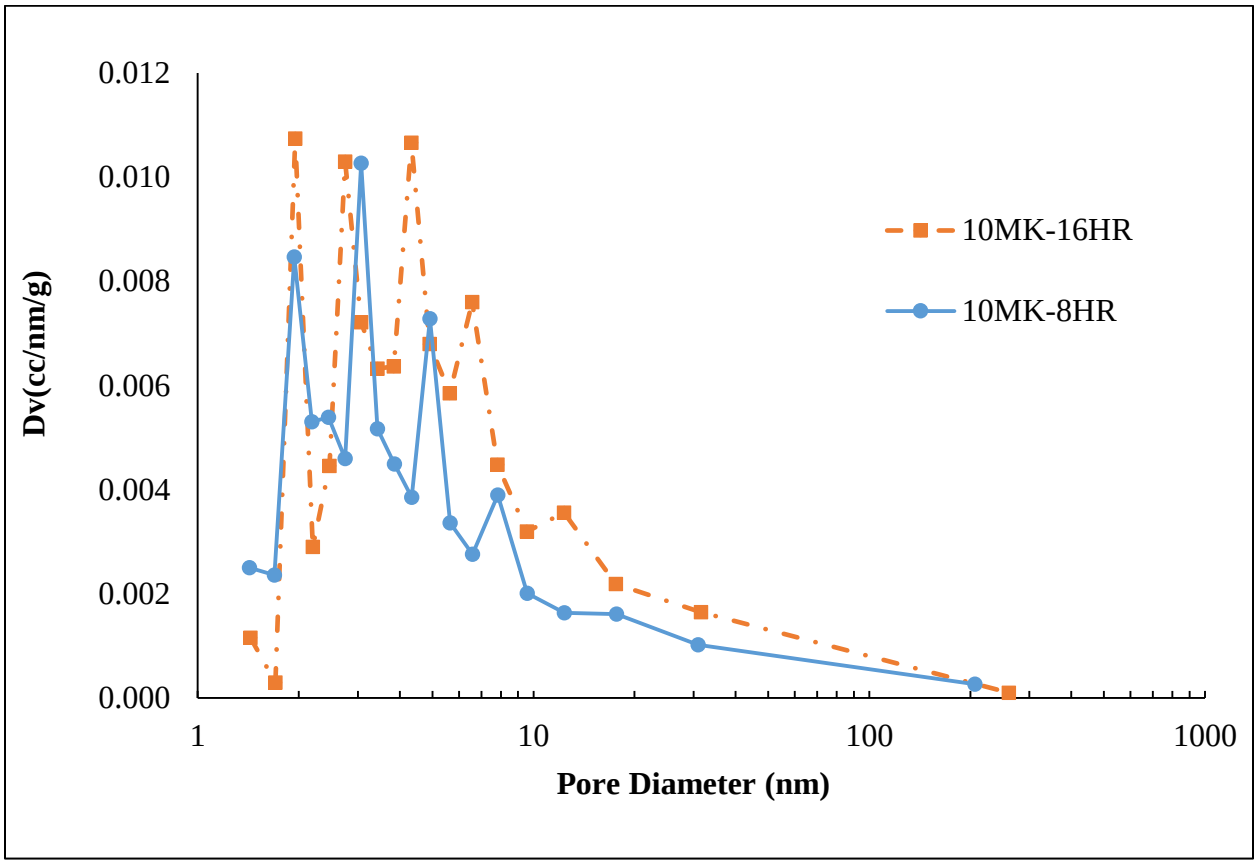

Figure 10: Comparison of Nitrogen Adsorption PSD for 10% Metakaolin at 8 and 16 hours

2.4.7 Rigid Cracking Frame

Both of the rigid cracking frame tests were conducted under non-isothermal conditions and their respective stress developments are shown in Figure 11.

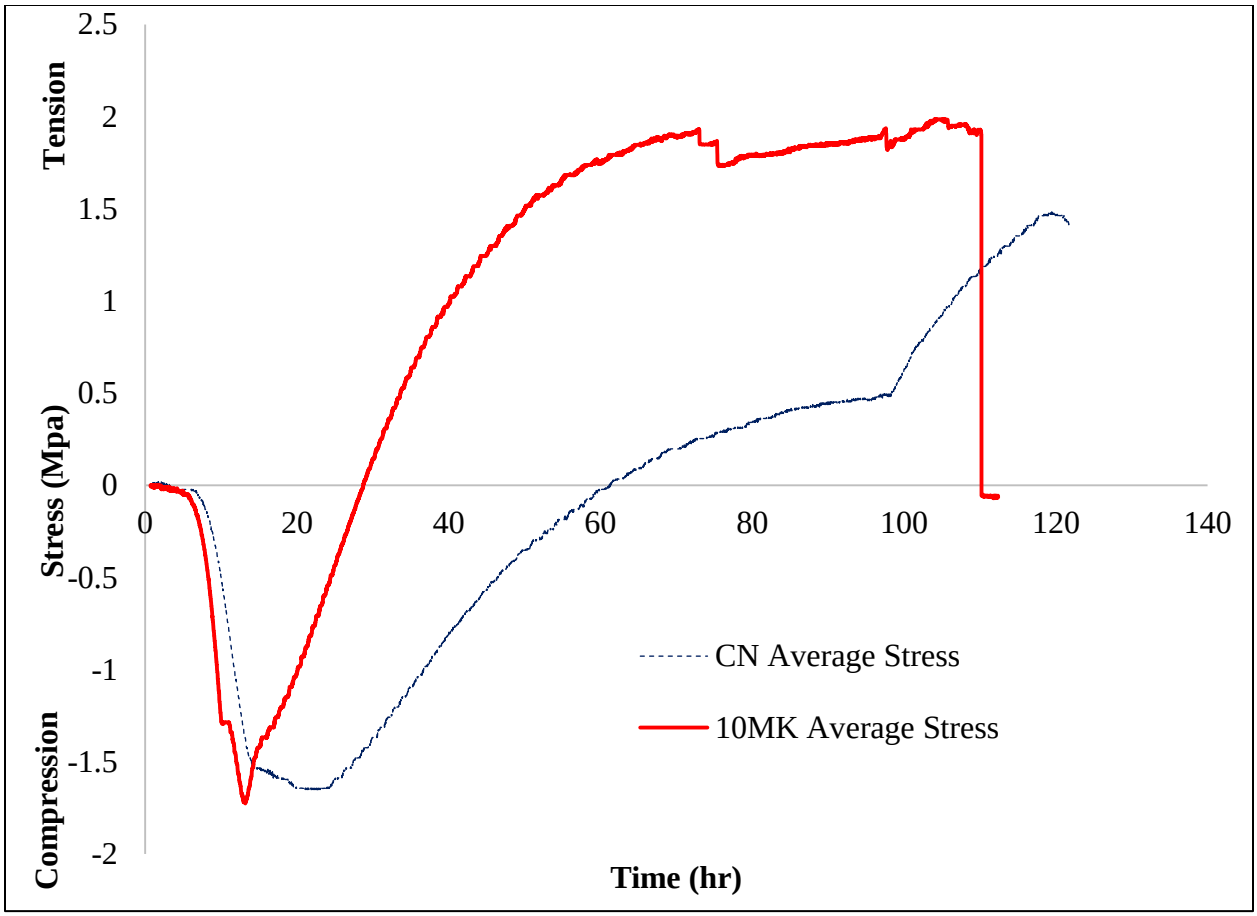

Figure 11. Stress evolution for 10MK and CN under stimulated temperature profile in the cracking frame

The inclusion of metakaolin increases the maximum compression stresses developed and shifted it to an earlier time. The time of zero stress was earlier by 31 hours when metakaolin was used. The tensional stress development of the 10MK increased at a higher rate and reached higher stresses than CN.

Thermal stress development is a combination of the coefficient of thermal expansion of the hardening concrete, the degree of restraint, temperature rise and stress relaxation [56]. By including metakaolin, the development of the elastic modulus of the concrete is higher than the CN mixture and in turn increases the elastic portion of the stress development. Additionally, the

higher heat of hydration of the 10MK mixture was likely responsible for much of the higher tensile stress development in the 10MK than the CN mixture.

The trends of the stress development in the rigid cracking frame mirror closely the strain present in the free shrinkage testing, both of which seem to be heavily influenced by the temperature profile that they were both exposed to. The rapid change from compressional to tensional stress is controlled by the switch from elongation to shrinkage. Due to 10MK experiencing a sharper temperature decrease, 10MK undergoes shrinkage and tensile stress development at a higher rate than CN. The sharp peaks in compressive stress development shown in the 10MK mixture between 11 and 15 hours are not seen in the free shrinkage tests and seem to be a unique feature of the mixture containing MK. The mechanism for this unusual stress behavior may be explained by the conversion of ettringite to Afm phases between 8 and 16 hours evidenced in the QXRD pattern. This reaction was shown in the porosity measurements and matched the volume change accompanying ettringite phase transformation. This volume change could cause a large increase in the stress-relaxation by placing higher stresses on other hydration products that did not undergo the reaction and were left to carry the load. This may not necessarily be picked up in a free shrinkage test, but would in a restrained stress test like the one performed. In spite of these differences between the early-age stress relaxation behavior of Portland cement concrete and concrete containing metakaolin, the B3 model was still able to model the stress development in concrete containing metakaolin as well as the control mixture.

2.4.8 Quantifying the Effect of Creep

Due to the constantly changing material properties of concrete in its early stages of development, many factors must be considered to accurately model its early age behavior. As the concrete ages, the elastic modulus develops, decreasing the relaxation effect that creep can have

on restraint stresses. An assumed strength based activation energy of 35,000 J/mol for 10MK and CN were used to help develop a working creep model. Figure 12 shows the stresses simulated in the rigid cracking frame using the measured free shrinkage results, the fit modulus development, and the modified B3 model, alongside the actual stress development of the concrete. The use of metakaolin was shown to reduce creep and the benefits associated with it, which is demonstrated by a lower magnitude of stress development to buffer the tensile stresses. The B3 model did an excellent job of modeling the stresses generated in the metakaolin cracking frame test, except for the peak between 11 and 16 hours. This is likely because of changes in the microstructure specific to MK that the model does not include. The model did an adequate job of modeling the CN mixture; however, at early ages either the strain was underestimated by the free shrinkage test, or the modulus at early ages was underestimated because of variability in the elastic modulus test.

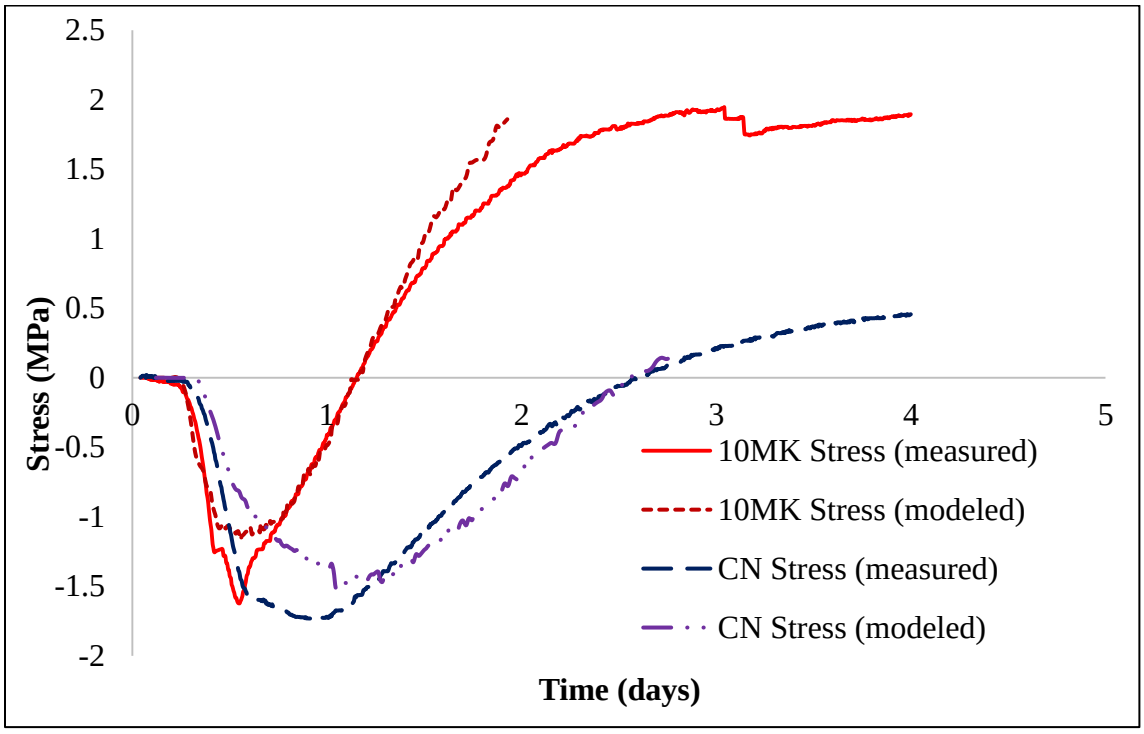

Figure 12. Modeled and measured stress development for 10MK and CN concrete

2.5 Conclusions

The findings of this study indicate that the use of metakaolin at 10% replacement levels rendered concrete more sensitive to cracking when mixtures were studied under temperature profiles simulating mass elements. This is due to the higher temperature sensitivity of mixtures incorporating metakaolin in addition to higher autogenous shrinkage. The control mixture has experienced more stress relaxation than metakaolin mixture. Preliminary studies indicate that phase transformation experienced by metakaolin can also be a contributing factor to metakaolin concrete mixtures higher temperature sensitivity. Reactions and conversion of Aft phases to Afm phases in metakaolin-containing mixtures increased the amount of pores and affected the stress relaxation behavior of the concrete mixture in ways not seen with the control mixture and not picked up in free shrinkage testing. In spite of these differences in behavior, the metakaolin concrete mixture early-age stress relaxation was able to be modeled by the modified B3 model.

2.6 Acknowledgements

This work has been partially supported by the Florida Department of Transportation and the Federal Highway Administration. The opinions are those of the authors and are not necessary those of the Florida Department of Transportation or US Department of Transportation.

2.7 References

[1] S. Mindess, *Cocnrete Second Edition*, 2nd ed. Prentice Hall, 2003.

[2] F. D. of Transportation, *STANDARD SPECIFICATIONS FOR ROAD AND BRIDGE CONSTRUCTION*. FDOT, 2015.

[3] J. Bai and S. Wild, “Investigation of the temperature change and heat evolution of mortar incorporating PFA and metakaolin,” *Cem. Concr. Compos.*, vol. 24, no. 2, pp. 201–209, 2002.

[4] J. Brooks and M. Johari, “Effect of metakaolin on creep and shrinkage of concrete,” *Cem. Concr. Compos.*, vol. 23, pp. 495–502, 2001.

[5] E. E. Holt, “Early age autogenous shrinkage of concrete,” University of Washington, 2001.

[6] E. G. Badogiannis, I. P. Sfikas, D. V. Voukia, K. G. Trezos, and S. G. Tsivilis, “Durability of metakaolin Self-Compacting Concrete,” *Constr. Build. Mater.*, vol. 82, pp. 133–141, 2015.

[7] Z. Shi, Z. Shui, Q. Li, and H. Geng, “Combined effect of metakaolin and sea water on performance and microstructures of concrete,” *Constr. Build. Mater.*, vol. 74, pp. 57–64, 2015.

[8] Z. ; Shi, M. R. G. Geiker, K. L. B. De Weerdt, K. Josef;, W. Kunther, S. Ferreiro, and J. Herfort, Duncan; Skibsted, *Durability of Portland Cement Blends Including Calcined Clay and Limestone: Interactions with Sulfate, Chloride and Carbonate Ions*, vol. 10. Dordrecht: Springer Netherlands, 2015.

[9] A. B. Hossain, S. Islam, and B. Reid, “A Comparative Study on Mortar Containing Silica Fume and High Reactivity Metakaolin in Relation to Restrained Shrinkage Stress Development and Cracking,” pp. 187–198.

[10] R. Springenschmid, R. Breitenbücher, and M. Mangold, “Development of the Cracking Frame and the Temperature-Stress Testing Machine,” in *RILEM Proceedings 25, Thermal Cracking in Concrete at Early Ages*, 1994, pp. 137–144.

[11] ASTM C1365, *Standard Test Method for Determination of the Proportion of Phases in Portland Cement and Portland-Cement Clinker Using X-Ray Powder Diffraction Analysis*, vol. Vol. 4.01, no. Reapproved. 2011, pp. 1–10.

[12] ASTM C204, *Standard Test Methods for Fineness of Hydraulic Cement by Air-Permeability Apparatus*. 2011.

[13] ASTM C188, *Standard Test Method for Density of Hydraulic Cement*. 2014, pp. 1–3.

[14] ASTM C1702, "Standard Test Method for Measurement of Heat of Hydration of Hydraulic Cementitious Materials Using Isothermal Conduction Calorimetry," *ASTM Int.*, pp. 1–7, 2009.

[15] J. L. Poole, K. a. Riding, K. J. Folliard, M. c. G. Juenger, and a K. Schindler, "Hydration Study of Cementitious Materials using Semi-Adiabatic Calorimetry," *Aci*, vol. SP 241, pp. 59–76, 2007.

[16] RILEM Technical Committee 119-TCE, "'Adiabatic and semi-adiabatic calorimetry to determine the temperature increase in concrete due to hydration heat of cement,'" 1998, pp. 451–464.

[17] A. K. Schindler and K. J. Folliard, "Heat of hydration models for cementitious materials," *ACI Mater. J.*, vol. 102, no. 1, pp. 24–33, 2005.

[18] K. a. Riding, J. L. Poole, K. J. Folliard, M. C. G. Juenger, and A. K. Schindler, "Modeling hydration of cementitious systems," *ACI Mater. J.*, vol. 109, no. 2, pp. 225–234, 2012.

[19] K. J. Folliard, M. Juenger, A. Schindler, J. Whigham, and J. L. Meadows, "Prediction Model for Concrete Behavior.," vol. 7, 2008.

[20] ASTM C403, “Standard Test Method for Time of Setting of Concrete Mixtures by Penetration Resistance,” *ASTM Int.*, pp. 1–7, 2008.

[21] ASTM C39, *Standard Test Method for Compressive Strength of Cylindrical Concrete Specimens*. 2012, pp. 1–7.

[22] ASTM C496, *Standard Test Method for Splitting Tensile Strength of Cylindrical Concrete Specimens*. 2011, pp. 1–5.

[23] ASTM C469, *Standard Test Method for Static Modulus of Elasticity and Poisson’ s Ratio of Concrete in Compression*. 2014, pp. 1–5.

[24] J. L. Meadows, “Early-age cracking of concrete structures,” p. 252, 2007.

[25] T. Meagher, N. Shanahan, D. Buidens, K. A. Riding, and A. Zayed, “Effects of chloride and chloride-free accelerators combined with typical admixtures on the early-age cracking risk of concrete repair slabs,” *Constr. Build. Mater.*, vol. 94, pp. 270–279, 2015.

[26] J. A. Whigham, “Evaluation of Restraint Stresses and Cracking in Early-Age Concrete with the Rigid Cracking Frame,” Auburn University, 2005.

[27] RILEM Technical Committee 119-TCE, “Development of the cracking frame at the temperature-stress testing machine,” in *Thermal Cracking in Concrete at Early Ages*, 1994.

[28] J. L. Poole and K. A. Riding, “Early Age Cracking : A Case Study in How Materials Modeling Can Improve Concrete Quality,” *Aci*, vol. SP 266-5, pp. 57–72, 2009.

[29] Z. P. Bazant and S. Baweja, “Creep and Shrinkage Prediction Model for Analysis and Design of Concrete Structures : Model B3 By Zden,” *Concr. Int.*, vol. 83, pp. 38–39, 2001.

[30] B. E. Byard and A. K. Schindler, “Modeling early-age stress development of restrained concrete,” *Mater. Struct.*, vol. 48, no. 1–2, pp. 435–450, 2013.

[31] D. MCHENRY, “a Lattice Analogy for the Solution of Stress Problems.,” *Journal of the ICE*, vol. 21, no. 2. pp. 59–82, 1943.

[32] F. Lagier and K. E. Kurtis, “Influence of Portland cement composition on early age reactions with metakaolin,” *Cem. Concr. Res.*, vol. 37, no. 10, pp. 1411–1417, 2007.

[33] M. Frías, M. I. S. De Rojas, and J. Cabrera, “The effect that the pozzolanic reaction of metakaolin has on the heat evolution in metakaolin-cement mortars,” *Cem. Concr. Res.*, vol. 30, no. 2, pp. 209–216, 2000.

[34] W. Lerch, *“ The Influence of Gypsum on the Hydration and Properties of Portland Cement Pastes ,”* vol. 46. 1946.

[35] D. Jansen, F. Goetz-Neunhoeffer, B. Lothenbach, and J. Neubauer, “The early hydration of Ordinary Portland Cement (OPC): An approach comparing measured heat flow with calculated heat flow from QXRD,” *Cem. Concr. Res.*, vol. 42, no. 1, pp. 134–138, 2012.

[36] C. Hesse, F. Goetz-Neunhoeffer, and J. Neubauer, “A new approach in quantitative in-situ XRD of cement pastes: Correlation of heat flow curves with early hydration reactions,” *Cement and Concrete Research*, vol. 41, no. 1. pp. 123–128, 2011.

[37] V. T. Cost, “Incompatibility of common concrete materials–influential factors, effects, and prevention,” in *Proceedings of the 2006 Concrete Bridge Conference*, 2006.

[38] J. P. Bombled, “Influence of sulfates on the rheological behavior of cement pastes and on their evolution,” in *7th International Congress on the Chemistry of Cement. Vol. 3*, 1980, p. Vi-164-169.

[39] K. a. Riding, J. L. Poole, A. K. Schindler, M. C. G. Juenger, and K. J. Folliard, “Effects of construction time and coarse aggregate on bridge deck cracking,” *ACI Mater. J.*, vol. 106, no. 5, pp. 448–454, 2009.

[40] J. L. Poole, K. a. Riding, K. J. Folliard, M. C. G. Juenger, and A. K. Schindler, “Methods for calculating activation energy for portland cement,” *ACI Mater. J.*, vol. 104, no. 1, pp. 86–94, 2007.

[41] K. A. Riding, J. L. Poole, A. K. Schindler, M. C. G. Juenger, and K. J. Folliard, “Quantification of effects of fly ash type on concrete early-age cracking,” *ACI Mater. J.*, vol. 105, no. 2, pp. 149–155, 2008.

[42] E. Güneyisi, M. Gesoğlu, S. Karaoğlu, and K. Mermerdaş, “Strength, permeability and shrinkage cracking of silica fume and metakaolin concretes,” *Constr. Build. Mater.*, vol. 34, pp. 120–130, 2012.

[43] S. Wild, J. M. Khatib, and A. Jones, “Relative Strength, Pozzolanic Activity and Cement Hydration in Superplasticised Metakaolin Concrete,” *Cem. Concr. Res.*, vol. 26, no. 10, pp. 1537–1544, 1996.

[44] P. Dinakar, P. K. Sahoo, and G. Sriram, “Effect of Metakaolin Content on the Properties of High Strength Concrete,” *Int. J. Concr. Struct. Mater.*, vol. 7, no. 3, pp. 215–223, 2013.

[45] A. Lotfy, O. Karahan, E. Ozbay, K. M. A. Hossain, and M. Lachemi, “Effect of kaolin waste content on the properties of normal-weight concretes,” *Constr. Build. Mater.*, vol. 83, pp. 102–107, 2015.

[46] R. Siddique and M. I. Khan, *Supplementary Cementing Materials*, vol. 37. Berlin, Germany: Springer Berlin Heidelberg, 2011.

[47] I. Dojkov, S. Stoyanov, J. Ninov, and B. Petrov, “On the consumption of lime by metakaolin, fly ash and kaoline in model systems,” *J. Chem. Technol. Metall.*, vol. 48, no. 1, pp. 54–60, 2013.

[48] C. S. Poon, S. C. Kou, and L. Lam, “Compressive strength, chloride diffusivity and pore structure of high performance metakaolin and silica fume concrete,” *Constr. Build. Mater.*, vol. 20, no. 10, pp. 858–865, 2006.

[49] E. Güneyisi, M. Gesoğlu, and K. Mermerdaş, “Improving strength, drying shrinkage, and pore structure of concrete using metakaolin,” *Mater. Struct.*, vol. 41, pp. 937–949, 2008.

[50] S. Wild, B. B. Sabir, J. Bai, and J. M. Kinuthia, “Self-compensating autogenous shrinkage in Portland cement—metakaolin—fly ash pastes,” *Advances in Cement Research*, vol. 12. pp. 35–43, 2000.

[51] P. J. P. Gleize, M. Cyr, and G. Escadeillas, “Effects of metakaolin on autogenous shrinkage of cement pastes,” *Cem. Concr. Compos.*, vol. 29, no. 2, pp. 80–87, 2007.

[52] F. M. Lea, *Lea: The Chemistry of Cement and Concrete*. 1970.

[53] B. Lothenbach, T. Matschei, G. Möschner, and F. P. Glasser, “Thermodynamic Modelling of the Effect of Temperature on the Hydration and Porosity of Portland Cement,” *Cem. Concr. Res.*, vol. 38, no. 1, pp. 1–18, 2008.

[54] K. Harada and H. Matsushita, “Effect of Gypsum Content in Cement on the Autogenous Shrinkage of Low-Heat Portland Blast Furnace Slag Cement,” *Memoris Fac. Eng. Univ.*, vol. 63, no. March 2003, pp. 51–66, 2003.

[55] P. Lura, Y. E. Guang, and K. Van Breugel, “Effect of Cement Type on Autogenous Deformation of Cement-Based Materials,” *ACI Spec. Publ.*, vol. 220, pp. 57–68, 2004.

[56] D. Buidens, “Effects of Mix Design Using Chloride-Based Accelerator on Concrete Pavement Cracking Potential,” University of South Florida, 2014.

[57] A. Williams, A. Markandeya, Y. Stetsko, K. Riding, and A. Zayed, “Cracking potential and temperature sensitivity of metakaolin concrete,” *Constr. Build. Mater.*, vol. 120, no. 2016, pp. 172–180, 2016.

CHAPTER 3: CONCLUSIONS AND FURTHER RESEARCH

In this study, the effect of incorporating metakaolin in concrete mixtures on the cracking potential was studied. This chapter presents the findings for this research and proposes recommendations for future studies.

The conclusions from this study are as follows:

1. Heat of hydration is drastically increased when using low replacement levels of metakaolin as shown by isothermal calorimetry and semi-adiabatic calorimetry.
2. The cracking potential of concrete utilizing metakaolin is increased, this is due to higher tensile stresses contributed from the combination of shrinkage from the hydration reaction and thermal effects.
3. Higher degrees of shrinkage are exhibited due to pore size refinement and a phase transformation, of which were testing using nitrogen absorption porosimetry and XRD.Utilizing metakaolin increases the compressive and splitting tensile strength of the concrete drastically during the initial stages of hydration.

The recommendations for future research are as follows:

1. Testing varying replacement levels of metakaolin with other SCMs to determine an optimal dosage level that does not compromise the likelihood of cracking.
2. Performing restrained ring tests with a temperature profile to determine how different restraints effect the probability and degree of cracking.

APPENDIX A: PERMISSION

Below is the permission from Elsevier to use the material in the Abstract and Chapter 2.

ELSEVIER LICENSE
TERMS AND CONDITIONS

Sep 20, 2016

This Agreement between Andrew Williams ("You") and Elsevier ("Elsevier") consists of your license details and the terms and conditions provided by Elsevier and Copyright Clearance Center.

License Number	3953230183264
License date	Sep 20, 2016
Licensed Content Publisher	Elsevier
Licensed Content Publication	Construction and Building Materials
Licensed Content Title	Cracking potential and temperature sensitivity of metakaolin concrete
Licensed Content Author	Andrew Williams,Ananya Markandeya,Yuriy Stetsko,Kyle Riding,A. Zayed
Licensed Content Date	1 September 2016
Licensed Content Volume Number	120
Licensed Content Issue Number	n/a
Licensed Content Pages	9
Start Page	172
End Page	180
Type of Use	reuse in a thesis/dissertation
Portion	full article
Format	both print and electronic
Are you the author of this Elsevier article?	Yes
Will you be translating?	No
Order reference number	
Title of your thesis/dissertation	Cracking Potential and Temperature Sensitivity of Metakaolin Concrete
Expected completion date	Oct 2016
Estimated size (number of pages)	50
Elsevier VAT number	GB 494 6272 12
Requestor Location	Andrew Williams 15107 roundup drive TAMPA, FL 33624 United States Attn: Andrew Williams
Total	0.00 USD
Terms and Conditions	